H₂ Production in the Radiolysis of Aqueous SiO₂ Suspensions and Slurries†

Jay A. LaVerne* and Sara E. Tonnies

Radiation Laboratory, University of Notre Dame, Notre Dame, Indiana 46556

Received: December 28, 2002

The production of H₂ in the radiolysis of silica suspensions in aqueous solutions and slurries has been examined. Radiation chemical yields of H₂ increase with increasing oxide weight fraction in suspensions of SiO₂ nanoparticles (7- and 22-nm diameter) probably because of the escape of electrons initially produced in the oxide to the bulk water. Reactions of H₂ with holes on the oxide surface or scavenging of precursors to H₂ in the bulk water decrease its yield at high SiO₂ loading. The production of H₂ in the radiolysis of slurries of large SiO₂ particles (8.1 m²/g, ∼343 nm diameter) is virtually identical to that expected in water alone suggesting little escape of electrons from the bulk oxide to the water. However, aqueous slurries of smaller SiO₂ particles (312 m²/g, ∼8 nm diameter) can double the H₂ production from water. Studies with varying the concentration of selenate, a good scavenger of the hydrated electron and its precursor, suggest that electron reactions on the μs time domain are responsible for the additional H₂ produced in aqueous SiO₂ mixtures. The only obvious difference between the 8-nm-particle slurry and the comparably sized suspension is the addition of additives in the latter for stability.

Introduction

Understanding radiation chemical effects at interfaces between solid materials and water presents many fundamental challenges with wide ranging practical applications. Catalytic effects in the radiolysis of suspensions of metallic particles in water have long been observed to increase molecular hydrogen production from the reducing species produced in water decomposition.[1−3] The primary deposition of energy by ionizing radiation in the different phases can lead to a variety of effects related to dosimetry involving boundaries. Equally important in the radiolysis of heterogeneous mixtures of water and solids is the migration of radiolytically produced excited species from one phase to another. There are also several very important practical reasons for radiolysis studies on water in association with solid surfaces. Water is in intimate contact with solid surfaces in the radiation fields of nuclear reactors and of wet nuclear waste materials in storage containers. Knowledge of the long-term radiation effects of these heterogeneous systems is of much technological interest.

There have been many radiolysis studies on water adsorbed on different surfaces concerned with H₂ production.[4−23] In all cases, the yield of H₂ was greater for water on the surface of a solid than for bulk water when the amount of energy directly deposited in the water is considered. The observation of an enhanced yield of H₂ in the radiolysis of adsorbed water has led to several proposed mechanisms for the transfer of energy from the solid material. Dissociative recombination of an electron−hole pair or dissociative electron attachment to a water molecule at the surface can lead to H₂ production.[24−27] Exciton formation in the bulk solid followed by diffusion and reaction at the surface may also be responsible for H₂ production from adsorbed water.[21−23] Very few radiation chemistry studies have been performed on systems in which water is the dominant component of the mixture. The pulse radiolysis of suspensions of silica nanoparticles in water with up to 50 wt % of the oxide finds an excess of hydrated electrons, but not holes, in the aqueous phase.[28,29] Combination reactions of hydrated electrons in water are a source of H₂ from irradiated bulk water.[30] Recent investigations have suggested that dissociative recombination reactions are also important for the production of H₂ from irradiated water.[31,32] Although excess electrons are observed in the radiolysis of silica nanoparticle suspensions, there has been no published work on the contribution of these electrons to excess H₂ formation. This work seeks to find a qualitative correlation between these two species in aqueous SiO₂ mixtures.

In this work, the formation of H₂ from the radiolysis of aqueous suspensions or slurries of SiO₂ was examined. The irradiations were performed with γ-rays, and the effects due to the variation in SiO₂ size and concentration were determined. An efficient scavenger for both the hydrated electron and its precursor was added to the aqueous slurries. The concentration of this scavenger was varied over a wide range to examine the temporal dependence of H₂ formation in heterogeneous silica/water mixtures.

Experimental Section

The aqueous colloidal suspensions were Dupont Ludox SM-30 and Dupont TM-50 obtained from Aldrich. The former is a 30 wt % ($\rho = 1.22$ g/cm³) suspension of 7-nm average-sized particles, and the latter is a 50 wt % ($\rho = 1.40$ g/cm³) suspension of 22-nm average-sized particles. Part of the SM-30 suspension was allowed to dry completely, and X-ray analysis suggested it was cristobalite, which has a density of 2.3 g/cm³. Perfect spheres have a specific area equal to $6/\rho d$, where ρ is the oxide density and d is the diameter. The predicted surface areas are 373 m²/g and 118 m²/g for the individual particles in SM-30 and in TM-50, respectively. The Ludox suspensions are at about pH 10. SM-30 solutions show intense light absorption at about 300 nm suggesting aromatic stabilizer additives. Solutions dialyzed for 2 days in sodium hydroxide at pH 10 show negligible absorption in this region. γ-radiolysis

---

* Address correspondence to this author.

was performed on Ludox solutions as received with 25 mM sodium nitrite added to inhibit back reactions of the OH radical with H_2. Dialyzed SM-30 solutions were not stable at high SiO_2 weight percent, but samples containing up to 15% oxide could be made and 25 mM sodium nitrite were irradiated.

Silica slurries were made by the addition of dry silica to ultrapure water obtained from a Millipore Milli-Q UV system. Fumed silica was obtained from Aldrich with a listed area of 380 m^2/g. Fused 325 mesh silicon (IV) dioxide powder was obtained from Alfa Aesar. BET surface area measurements were determined on a Quantachrome Autosorb 1 analyzer. This instrument operates by measuring nitrogen adsorption and desorption from the surface at an equilibrium vapor pressure using the BET (Brunauer–Emmet–Teller) method of surface area calculation. Specific areas of the powders were determined to be 312 and 8.1 m^2/g for the fumed and fused 325 mesh silica, respectively. These areas correspond to average diameters of 8 and 343 nm, respectively, assuming spherical particles. γ-irradiations were performed on slurries obtained by the addition of a given weight of silica to 2 mL of 1 mM KBr (Fisher Scientific) solutions containing various concentrations of sodium selenate decahydrate (Aldrich). The Br^- was added to suppress OH radical back reactions with H_2 and the SeO_4^{2-} was added as a scavenger of dry and hydrated electrons.

Radiolysis with γ-rays was performed using a Shepherd 109 ^{60}Co source at the Radiation Laboratory of the University of Notre Dame. The dose rate was about 150 Gy/min as determined using the Fricke dosimeter.[33] The sample cell for the suspensions was made from a 1-cm quartz cuvette with inlet and outlet ports for purging the sample before and after irradiation. A 0.2-μm PTFE membrane was epoxy sealed near the outlet port to prevent foaming liquid from being transported into the gas chromatograph. All fittings and the membrane were out of the radiation field. The same cuvette was used for both dosimetry and sample irradiation. Energy absorbed by the suspensions was obtained from the dosimetry and corrected for the weight of the water and silica mixture in the sample cell. Slurry samples were degassed with argon and flame sealed in 1-cm diameter Pyrex tubes 10-cm long. Samples were rotated at 1 rpm throughout the irradiation to ensure complete mixing of the particles and water. Dosimetry in the slurries was performed relative to the 2-mL aqueous solution present in all samples, that is, radiation chemical yields were determined with respect to the energy absorbed by the water only.

Hydrogen from radiolysis of the suspensions was determined using an inline technique with a gas chromatograph. Ultrahigh purity argon was used as the carrier gas with a flow rate of about 50 mL/min. The argon passed through a constant flow regulator, an injection septum, and a four-way valve and into a 3-m 5x molecular sieve column of an SRI 8610C gas chromatograph with a thermal conductivity detector. The sample was connected to the gas analysis system using the four-way valve, purged of air, isolated, irradiated, and then injected into the carrier gas stream. Hydrogen was determined in the slurry samples by placing the irradiated samples in a section of Tygon tubing isolated from the gas chromatograph carrier gas with a four-way valve. The irradiated sample was placed in the Tygon tubing, purged, and isolated by the four-way valve. The sample cell was crushed and then injected into the carrier gas stream. Calibration of the gas chromatograph was performed by injecting pure gases with a gastight microliter syringe. Error in gas measurement is estimated to be about 5%.
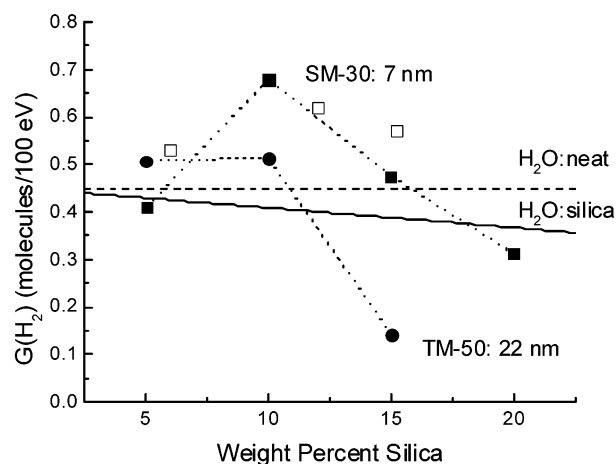

Figure 1. Production of H_2 in aqueous suspensions of SiO_2 with 25 mM NO_2^- as a function of the weight percent of oxide: (■) Ludox SM-30 (7-nm diam), (●) Ludox TM-50 (22-nm diam), (□) dialyzed Ludox SM-30. The dashed line is the H_2 yield in water with 25 mM NO_2^- and no oxide. The solid line is the expected yield of H_2 in 25 mM NO_2^- because of energy deposition in the oxide.

Results and Discussion

SiO_2 Suspensions. Experiments were performed on suspensions of SiO_2 nanoparticles in order to have a direct comparison between H_2 yields and previous measurements of hydrated electron production.[28] Figure 1 gives the radiation chemical yields of H_2 as a function of the weight percent of silica in various solutions of SM-30 and TM-50. Radiation chemical yields, G-values, are given in units of number of molecules of H_2 formed per 100 eV of total energy adsorbed. For the suspensions, the total energy is the amount of energy absorbed by both the oxide and water. Nitrite anion was added to the suspensions (25 mM) to prevent back reaction of the OH radicals with H_2 and to stop long-time combination reactions of hydrated electrons and H atoms. Therefore, the G-values reported here represent the yields on the μs time scale. The corresponding H_2 yield in solutions without added oxide is 0.45 molecules/ 100 eV as shown by the dashed line in Figure 1. With increasing mass of silica, there is an increase in deposition of energy in the solid phase compared to the water. H_2 yields are expected to decrease with increasing silica fraction according to the solid line in Figure 1 if there is no interaction between the phases. Any deviation in the H_2 yields from the solid line represents changes in the chemistry because of oxide–water interactions.

Molecular hydrogen yields at low weight percent silica suspensions agree with the values in neat water. The yields of H_2 increase with the addition of silica until about 10 wt % and then decrease at higher silica fractions. The increase in H_2 is more pronounced in SM-30 than in TM-50. There is more than a 50% maximum increase in the yields in SM-30 at about 10 wt % suggesting that excess precursors to H_2 are being produced in the radiolysis of water with added oxide. The nature of the precursor cannot be determined from these experiments, but it is presumably the hydrated electron that is observed in excess in the pulse radiolysis experiments.[28] The larger yield of H_2 with SM-30 than with TM-50 may be due to its smaller size, which facilitates electron ejection into the bulk water. However, other processes related to the degradation of H_2 may also be responsible for the differences in yield.[34]

At high silica fractions, the yield of H_2 decreases with increasing silica weight percent. This decrease is more than that expected because of the fraction of energy loss in the solid particles alone. Similar results were observed in the radiolysis
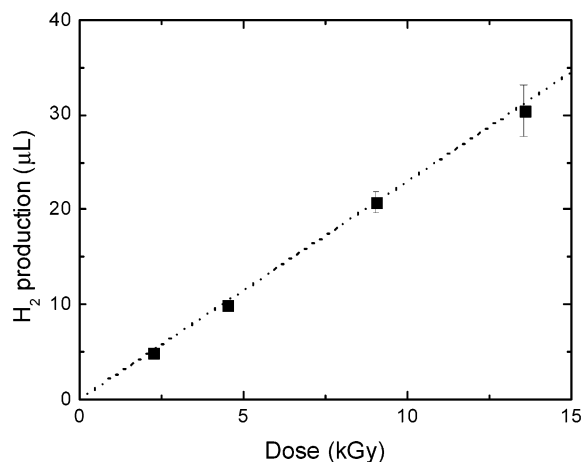
H$_2$ Production in the Radiolysis of Aqueous SiO$_2$

J. Phys. Chem. B, Vol. 107, No. 30, 2003 **7279**

Figure 2. Dose dependence of H$_2$ yield in aqueous slurry of fused 325 mesh SiO$_2$ (8.1 m^2/g) with 1 mM SeO$_4^{2-}$ and 1 mM Br$^-$.

Figure 3. Production of H$_2$ in aqueous slurries of SiO$_2$ with 1 mM SeO$_4^{2-}$ and 1 mM Br$^-$: (●) fused 325 mesh SiO$_2$ (8.1 m^2/g) and (■) fumed SiO$_2$ (312 m^2/g). The dotted line is the H$_2$ yield in water with 1 mM SeO$_4^{2-}$ and 1 mM Br$^-$ but no oxide.

of SiO$_2$ suspensions with added ferricyanide and ferrocyanide.[34] That work attributed the lower than expected yields to a back reaction of the H$_2$ and the trapped holes at the surface of the solid particles. Such a process is thought to be energetically possible but not yet confirmed. Those researchers performed further experiments in the presence of 1 mM Ru(NH$_3$)$_6^{2+}$, which adsorbs on the surface of the particles. The divalent state or this ruthenium cation reacts with hole and the H$_2$ yields are observed to decrease with increasing silica fraction at the rate expected because of energy fractionation between the two phases.

Another possible reason for the large decrease in yields at high silica fractions may be the scavenging of the precursors to H$_2$ by impurities in the Ludox solutions. Strong absorbance peaks at 300 nm suggest that an aromatic organic may be present in these solutions as a stabilizer. Dialysis of SM-30 suspensions removed all traces of these peaks, but the resultant suspensions are not stable at high SiO$_2$ concentrations. Nonetheless, γ-radiolysis experiments performed on dialyzed SM-30 solutions yield results that are similar to those for undialyzed solutions. The maximum concentration of SiO$_2$ in the dialyzed solutions is too low to definitely eliminate the possible role of impurities in the water phase. Further experiments are necessary to examine this problem more thoroughly.

SiO$_2$ Slurries. Aqueous slurries of SiO$_2$ were made by the addition of oxide to a fixed volume of an aqueous solution. The volume of the liquid was 2 mL in all of the experiments, and radiation chemical yields were determined relative to the energy absorbed by the water alone. Presentation of the H$_2$ yields in this manner makes it easier to compare the results with oxides to that for the aqueous solution alone. This mode of comparison is especially suitable for the scavenger concentration studies to be discussed below.

Figure 2 shows the production of H$_2$ as a function of the dose to the water for slurries of 0.5 g of fused 325 mesh SiO$_2$ (8.1 m^2/g) with 1 mM SeO$_4^{2-}$ and 1 mM Br$^-$. The response is linear from 2 to 14 kGy. Higher doses will lead to a significant depletion of the solutes with a deviation from linearity because of long-time radical reactions with stable products. The linearity suggests that there is negligible buildup of transient products, such as holes on the surface, which may react with H$_2$ or its precursor.

A series of experiments were performed to examine the dependence of H$_2$ yields on the fraction of SiO$_2$ loading. The slurries had a wide range of viscosities depending on the oxide fraction and the particle size. High concentrations of fumed SiO$_2$
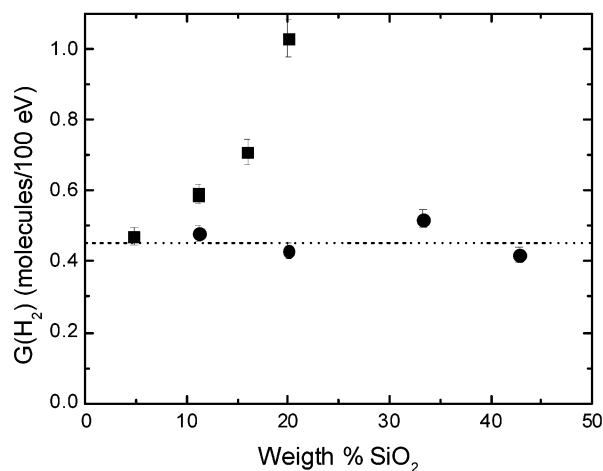
(312 m^2/g) particles were almost solid because of the bonding between particles. The reported yields in these systems may be lower limit values because it was difficult to ensure complete mixing of the water and oxide during the radiolysis. Figure 3 shows the results for H$_2$ yields as a function of the weight percent of added SiO$_2$ to the 2 mL of water. Fused 325 mesh SiO$_2$ (8.1 m^2/g) has virtually no effect on H$_2$ yield at all values of oxide loading. Monte Carlo calculations predict that the average energy loss in a collision of a 1 MeV electron in liquid water is about 57 eV so most secondary electrons will be formed with a kinetic energy of about 50 eV.[35] Comparable calculations for SiO$_2$ suggest a somewhat similar value for the average energy of the secondary electrons. (Pimblott, S. M., University of Notre Dame, 2003). The range of low-energy electrons in condensed phases is particularly difficult to measure or predict, but the ICRU continuous slowing down approximation, csda, range value for 50 eV electrons in water is 2.85×10^{-7} g/cm^2.[36] The csda range represents the path length of the electron. Scaling to the density of SiO$_2$ gives a range of only 1.2 nm. The fused 325 mesh SiO$_2$ particles are relatively large ($\sim$343 nm diameter) and most of the secondary electrons produced in them can be expected to remain trapped in the particle. However, the smaller fumed SiO$_2$ particles (312 m^2/g) have an average diameter of only about 8 nm and a large fraction of the low-energy electrons produced in the oxide by the direct absorption of energy by the γ-rays are expected to escape into the water layers. The results for the fumed SiO$_2$ slurries (312 m^2/g) in Figure 3 show a large increase in H$_2$ yield with the addition of oxide. At the level of 0.5 g of oxide to 2 mL of aqueous solution (20 wt %), the H$_2$ yield is more than double that of the aqueous solution alone.

The γ radiolysis of liquid water leads to the production of H$_2$ by several different mechanisms. Scavenger studies show that a major fraction of the total formation of H$_2$ in the nonhomogeneous chemistry following the passage of ionizing radiation is due to precursors of the hydrated electron.[31,32] Most of the rest of the formation of H$_2$ is due to reactions of the hydrated electron and H atoms.[30] At about 1 μs following the passage of a γ-ray, the track or string of spurs induced by the radiation has dissipated and the radiolytic products are homogeneously distributed in the medium. The yield of H$_2$ implied in the previous discussion corresponds to about 1 μs where the spur chemistry is virtually complete and bulk or long-time chemistry begins to occur. Increasing the concentration of scavengers for the precursor to H$_2$ allows one to probe the
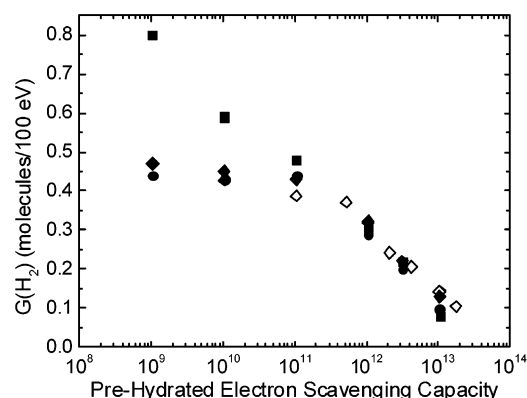
Figure 4. Yield of H_2 in aqueous slurries of SiO_2 with 1 mM Br^- as a function of SeO_4^{2-} concentration: (●) fused 325 mesh SiO_2 (8.1 m^2/g), (■) fumed SiO_2 (312 m^2/g), (◆) no oxide, and (◇) no oxide, ref 31.

kinetics of its formation because of the competition of the first-order scavenging reaction with the second-order spur reactions.

The yields of H_2 are shown in Figure 4 as a function of the scavenging capacity of the selenate solute for the prehydrated electron. The scavenging capacity is the product of the selenate concentration and the rate coefficient for the scavenging reaction with the precursor to the hydrated electron (1.05 × 10^{13} M^{-1} s^{-1})[31,32] The lifetime of the prehydrated electron is approximately equal to the inverse of the scavenging capacity. It can be seen in Figure 4 that the results for fused 325 mesh SiO_2 (8.1 m^2/g) slurries at 0.5 g/2 mL closely follow the results of aqueous solutions alone. At high-scavenging capacity (short times), the results with fumed SiO_2 (343 m^2/g) slurries are also similar to that of aqueous solutions alone, but at longer times (lower-scavenging capacity) the H_2 yields increase significantly in these mixtures. The short-time chemistry in the γ-radiolysis of liquid water is due to intraspur reactions of radicals and ions formed in close proximity to each other. Electrons escaping the oxide particles are not expected to have this close spatial correlation since the corresponding holes are believed to remain in the solid.[29] Reactions of these excess electrons with each other to produce H_2 are not expected to be on the same time scale as the dissociative combination reactions occurring in the spur. The combination reactions of near homogeneously distributed hydrated electrons are expected to occur on the μs time domain in agreement with the observed results. Future experiments using scavengers with different reactivity toward the hydrated electron and its precursor may be able to give more information on their kinetics, which can then be used to determine number and distribution of electrons about the oxide.

Conclusions

These experiments have examined the production of H_2 in the radiolysis of aqueous suspensions and slurries of SiO_2. Radiation chemical yields of H_2 seem to increase with increasing oxide fraction in the suspensions. This increase is thought to be due to escape of electrons initially produced in the oxide to the bulk water. At high SiO_2 loading, reactions of radiolytic transients with H_2 or impurities with its precursor lead to the observed decease in H_2 yield. The production of H_2 in the radiolysis of SiO_2 slurries shows virtually no difference between aqueous solutions and added oxide using large fused 325 mesh SiO_2 particles (8.1 m^2/g, ~343 nm diameter). However, aqueous slurries of smaller fumed SiO_2 particles (312 m^2/g, ~8-nm diameter) show a marked increase in H_2 production from aqueous solutions alone. The only obvious difference between

the 8-nm-particle slurry and the comparably sized suspension is the addition of stabilizers in the latter. Studies varying the concentration of the prehydrated electron scavenger suggest that electron reactions on the μs time domain are responsible for the extra production of H_2.

References and Notes

(1) Henglein, A. *Ber. Bunsen-Ges. Phys. Chem.* **1977**, *81*, 556.
(2) Henglein, A. *J. Phys. Chem.* **1979**, *83*, 2209.
(3) Meisel, D. *J. Am. Chem. Soc.* **1979**, *101*, 6133.
(4) Garibov, A. A.; Melikzade, M. M.; Bakirov, M. Ya.; Ramazanova, M. Kh. *High Energy Chem.* **1982**, *16*, 101.
(5) Rustamov, V. R.; Bugaenko, L. T.; Kurbanov, M. A.; Kerimov, V. K. *High Energy Chem.* **1982**, *16*, 148.
(6) Garibov, A. A.; Melikzade, M. M.; Bakirov, M. Ya.; Ramazanova, M. Kh. *High Energy Chem.* **1982**, *16*, 177.
(7) Garibov, A. A. Proceedings of the Fifth Symposium on Radiation Chemistry; Dobo, J., Hedvig, P., Schiller, R., Eds.; Akademiai Kiado: Budapest, 1983; p 377.
(8) Garibov, A. A.; Bakirov, M. Ya.; Velibekova, G. Z.; Elchiev, Ya. M. *High Energy Chem.* **1984**, *18*, 398.
(9) Nechaev, A. *Radiat. Phys. Chem.* **1986**, *28*, 433.
(10) Aleksandrov, A. B.; Gusev, A. L.; Petrik, N. G. *Russ. J. Phys. Chem.* **1987**, *61*, 102.
(11) Garibov, A. A.; Gezalov, Kh. B.; Velibekova, G. Z.; Khudiev, A. T.; Ramazanova, M. Kh.; Kasumov, R. D.; Agaev, T. N.; Gasanov, A. M. *High Energy Chem.* **1987**, *21*, 416.
(12) Nakashima, M.; Tachikawa, E. *J. Nucl. Sci. Technol.* **1987**, *24*, 41.
(13) Gezalov, K. B.; Gasanov, A. M.; Garibov, A. A.; Abdullayeva, K. I. *Radiat. Phys. Chem.* **1988**, *32*, 615.
(14) Garibov, A. A.; Velibekova, G. Z.; Kasumov, R. D.; Gezalov, Kh. B.; Agaev, T. N. *High Energy Chem.* **1990**, *24*, 174.
(15) Garibov, A. A.; Parmon, V. N.; Agaev, T. N.; Kasumov, R. D. *High Energy Chem.* **1991**, *25*, 86.
(16) Garibov, A. A.; Agaev, T. N.; Kasumov, R. D. *High Energy Chem.* **1991**, *25*, 337.
(17) Aleksandrov, A. B.; Bychkov, A. Yu.; Vall, A. I.; Petrik, N. G.; Sedov, V. M. *Russ. J. Phys. Chem.* **1991**, *65*, 847.
(18) Garibov, A. A.; Velibekova, G. Z.; Agaev, T. N.; Dzhafarov, Ya. D.; Gadzhieva, N. N. *High Energy Chem.* **1992**, *26*, 184.
(19) Nakashima, M.; Aratono, Y. *Radiat. Phys. Chem.* **1993**, *41*, 461.
(20) Nakashima, M.; Masaki, N. M. *Radiat. Phys. Chem.* **1996**, *47*, 241.
(21) Petrik, N. G.; Alexandrov, A. B.; Orlando, T. M.; Vall, A. I. *Trans. Am. Nucl. Soc.* **1999**, *81*, 101.
(22) Petrik, N. G.; Alexandrov, A. B.; Vall, A. I. *J. Phys. Chem. B* **2001**, *105*, 5935.
(23) LaVerne, J. A.; Tandon, L. *J. Phys. Chem. B* **2001**, *105*, 9316.
(24) LaVerne, J. A.; Pimblott, S. M. *J. Phys. Chem. A* **2000**, *104*, 9820.
(25) Rowntree, P.; Parenteau, L.; Sanche, L. *J. Chem. Phys.* **1991**, *94*, 8570.
(26) Kimmel, G. A.; Orlando, T. M.; Vezina, C.; Sanche, L. *J. Chem. Phys.* **1994**, *101*, 3282.
(27) Cobut, V.; Jay-Gerin, J.-P.; Frongillo, Y.; Patau, J. P. *Radiat. Phys. Chem.* **1996**, *47*, 247.
(28) Schatz, T.; Cook, A. R.; Meisel, D. *J. Phys. Chem. B* **1998**, *102*, 7225.
(29) Dimitrijevic, N. M.; Henglein, A.; Meisel, D. *J. Phys. Chem. B* **1999**, *103*, 7073.
(30) Allen, A. O. *The Radiation Chemistry of Water and Aqueous Solutions*; Van Nostrand: New York, 1961.
(31) Pastina, B.; LaVerne, J. A.; Pimblott, S. M. *J. Phys. Chem. A* **1999**, *103*, 5841.
(32) LaVerne, J. A.; Pimblott, S. M. *J. Phys. Chem. A* **2000**, *104*, 9820.
(33) Pastina, B.; LaVerne, J. A. *J. Phys. Chem. A* **1999**, *103*, 1592.
(34) Miyoshi, H.; Schatz, T.; Meisel, D. to be published.
(35) Pimblott, S. M.; LaVerne, J. A.; Mozumder, A. *J. Phys. Chem.* **1996**, *100*, 8595.
(36) *Linear Energy Transport*; ICRU Report 16; International Commission on Radiation Units and Measurements: Washington, DC, 1970.